ВІСНИК ЛЬВІВ. УН-ТУ
Серія фіз. 2009. Вип. 43. С. 126–134

VISNYK LVIV UNIV.
Ser. Physics. 2009. Is. 43. P. 126–134

PACS number(s): 61.20.Lc, 64.70.Pf

STUDY OF THE INFLUENCE OF CRYSTALLIZATION ON THE PROPERTIES OF Fe-Si-B METALLIC GLASS

M. Jakubczyk[1], P. Siemion[1], L. Krajczyk[2], E. Jakubczyk[3]

[1]*Institute of Chemistry and Environmental Protection, Jan Długosz University*
Al. Armii Krajowej 13/15, 42-200 Częstochowa, POLAND
[2]*W. Trzebiatowski-Institute of Low Temperature and Structure Research*
Polish Academy of Sciences, Okolna 2, 50-950 Wrocław, POLAND
[3]*Institute of Physics, Jan Długosz University*
Al. Armii Krajowej 13/15, 42-200 Częstochowa, POLAND
e-mail: e.jakubczyk@ajd.czest.pl

The investigations of the crystallization process of $Fe_{78}Si_9B_{13}$ metallic glass performed by DSC, X-ray diffraction, electrical resistivity, Hall effect and TEM methods. As result of these measurements two-stages crystallization was stated. By means of non-isothermal DSC experiments the activation energy and the Avrami exponent were determined for both stages. The created phases: α-Fe(Si) and $(Fe,Si)_2B$ were identified on the basis of X-ray and TEM investigations. However, TEM observations showed also a little amount of the FeB_{49} phase as well as some rest of the amorphous phase. The electrical and Hall resistivities decrease abruptly after the creation of the phases out of the amorphous matrix.

Key words: metallic glass, crystallization, activation energy, Avrami exponent, electrical and Hall resistivities.

The amorphous structure of metallic glasses is metastable state. This metastability is understandable, because the solid state is obtained as result of rapid cooling of a liquid alloy. Therefore the metallic glasses possess a liquid structure, and they are very defective, mainly because of free volumes that are created. Besides, a higher energetic state is established, because atoms, during the quick transition from the liquid to the solid state, do not take up an equilibrium position, in which they would have lower energy. As a result the metallic glasses undergo structural relaxations. The structural relaxations, involving atom rearrangements, modify the short range order. These modifications lead to changes within the chemical or/and topological short range ordering, later on through the changes in the intermediate state with the medium range order leading finally to the polycrystalline state with the long range order. For the application purposes of the metallic glasses, the investigations explaining the crystallization mechanisms are performed. The knowledge of these mechanisms could be used to control the crystallization process and determine the intervals of the efficient metallic glass applications, as well as, to obtain some special structures, either partially or completely crystalline, which cannot be obtained direct from the liquid state.

This paper present the investigations of the thermally stimulated modification of the structural order of $Fe_{78}Si_9B_{13}$ metallic glasses by the methods: the non-isothermal differential scanning calorimetry (DSC), the X-ray diffraction (XRD), Hall and electrical resistivities and transmission electron microscopy (TEM). The annealing of the samples was performed isochronally (4h) at different temperatures to obtain the complete crystallization.

The metallic glass $Fe_{78}Si_9B_{13}$ was prepared by the roller quenching method in Institute of Materials Engineering of Warsaw Technical University, Poland.

Continuous heating DSC experiments were carried out using STA-409C NETZSCH apparatus. Heating rates of 5, 10, 15 and 20 K/min were used. The scanned temperature from room temperature up to 900 K and temperature precision was $\pm$ 0,1 K. High purity argon was used as inert atmosphere. The mass of sample was typically (22–25 mg).

X-ray diffraction were done at room temperature for the as-received as well as isochronally (4 h) annealed samples at various temperatures (573-823 K). The X-ray studies were performed using a DRON-2,0 diffractometer with a horizontal goniometer of GUR-5 type. The X-ray tube had a molybdenium target $\left(\lambda_{K\alpha} = 0,71069 \cdot 10^{-10} m\right)$ and a graphite monochromator in the primary beam.

The Hall voltage was measured by a constant current method in the field up to 3.26 T. The electrical resistivity was also measured within d. c. regime. The samples for the measurements of the Hall and electrical resistivities were prepared by selective etching using photolithography.

The microstructure and phase composition were studied by transmission electron microscopy (TEM), high resolution transmission electron microscopy (HRTEM) and selected area electron diffraction (SAED) methods with Philips CM 20 Super Twin microscope, which at 200 kV provides 0,24 nm resolution. Specimens for TEM and HRTEM were prepared by grinding the samples in mortar and dispersing in methanol with ultrasonic agitation. A droplet of suspension was deposited on a microscope grid covered with carbon film.

In order to determine the activation energy of crystallization process of $Fe_{78}Si_9B_{13}$ metallic glass DSC method was applied. The measurements of non-isothermal crystallization were carried out at the continuous heating rates of 5, 10, 15 and 20 K/min. All the DSC curves display two clearly separate exothermic peaks. The position on the temperature axis of both peaks put forward with the increase of the heating rate. It allows that the transformation from the amorphous to the crystalline state proceeds through two main stages. Knowledge the peaks of the temperature allows to determine the activation energy E_a for the crystallizing phases according to the Kissinger equation [1, 2]:

$$\ln\left(\beta / T_p^2\right) = -E_a / RT_p + \ln\left(K_0 R / E_a\right), \tag{1}$$

(where: $\beta = dT / dt$ is heating rate, T_p peak of the temperature, R the gas constant and K_0 frequency factor).On the basis of the Kissinger plots: $\ln\left(\beta / T_p^2\right)$ vs. $1/T_p$ for both stages the values E_a are received from the approximately straight line by least-squares fitting. The calculated values are listed in table 1.

The isothermal solid state transformation is strictly described by the Johnson-Mehl-Avrami (JMA) equation [3]:

$$x(t) = 1 - \exp\left[-(Kt)^n\right], \tag{2}$$

where: x is the volume fraction transformed after time t, n a dimensionless quantity called the kinetics exponent, and K the reaction rate constant. The temperature dependence of K is generally expressed by the Arrhenius equation:

$$K(T) = K_0 \exp(-E_a / RT). \tag{3}$$

However, it is very interesting to generalize of the JMA equation to experiments in which the rate of heating $\beta = dT/dt$ is constant. Assuming that progress of crystallization and mechanism do not change with temperature, the volume fraction transformed after time t is described as [2]:

$$x(t) = 1 - \exp\left[-\left(\int_0^t K\left[T(t')\right]dt'\right)^n\right] = 1 - \exp\left(-I^n\right), \tag{4}$$

where: $K\left[T(t')\right]$ is expressed by the Arrhenius formula (3), $T(t')$ is the temperature at the time t'.

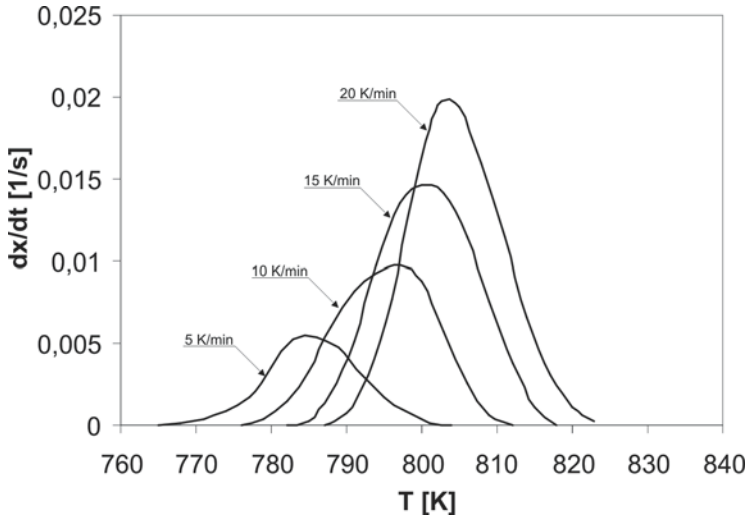

Fig. 1. Crystallization rate, dx/dt, vs. temperature, T, for the $Fe_{78}Si_9B_{13}$ metallic glass at different heating rates for the first stage of crystallization

The determination of the maximum crystallization rate from equation (4) leads to:

$$nK_p\left(I^n\right)_p = \beta E I_p / RT_p^2 + (n-1)K_p, \tag{5}$$

(where subscript p denotes the magnitude values at the maximum crystallization rate).

The integral I can be represented by the alternating series and thus it is obtained [2]:

$$I = RT^2 K(\beta E_a)^{-1}\left(1 - 2\frac{RT}{E_a}\right). \tag{6}$$

Because, almost always: $E_a / RT \rangle\rangle 1$ (usually $E_a / RT \geq 25$) then for the maximum crystallization rate

$$I = I_p = RT_p^2 K_p \left(\beta E_a\right)^{-1} \tag{7}$$

and on the base (6) $I_p = 1$.

Finally, the kinetics exponent n is described by the equation

$$n = \left(dx / dt\right)_p RT_p^2 \left(0{,}37\beta E_a\right)^{-1}. \tag{8}$$

Although the JMA equation was deduced for the isothermal case, it is widely applied also by many authors to the non-isothermal crystallization process [2–6]. The JMA equation is used in a variety of mathematical analysis of the non-isothermal solids state transformation. Here, we calculated the Avrami kinetics exponent n from the equation (8) developed at the first time by Y. Q. Gao and W. Wang [3].

The crystallized fraction x at any temperature T is given as $x = A_x/A$, where A and A_x are total and part (at generic temperature T) area of exoterm peak, respectively. The crystallization rates versus temperature for first stage are presented in fig. 1. The maximum crystallization $(dx/dt)_p$ for each heating rate gives n, according to the equation (8). Mean values of the kinetics exponent n are included in table 1. The values n indicate that at the first and second stages of the crystallization process there are crystal growth controlled by diffusion and by interface, respectively [7].

Table 1

The activation energy E_a and the Avrami kinetics exponent n for both stages of crystallization of the $Fe_{78}Si_9B_{13}$ metallic glass and of elementary cells of created phases

Parameters	I stage	II stage
E_a [kJ/mol]	341	410
n	2,49	4,93
phase	α – Fe(Si) cubic ($Im\bar{3}m$) a = 2,856 Å	$(Fe, Si)_2B$ tetragonal (I4/mcm) a = 5,105 Å c = 4,228 Å

In order to identify the crystalline phases formed in the amorphous matrix the X-ray and TEM investigations were performed. The investigations of the X-ray diffraction prove that the first and second stages of the crystallization occur after the annealing at the temperature 723 and 773 K, respectively. By means of the qualitative analysis it was established that at the first and second stages are formed α-Fe(Si) and $(Fe,Si)_2B$ phases, respectively [8–9]. The parameters of the elementary cells of the created phases are listed in table 1.

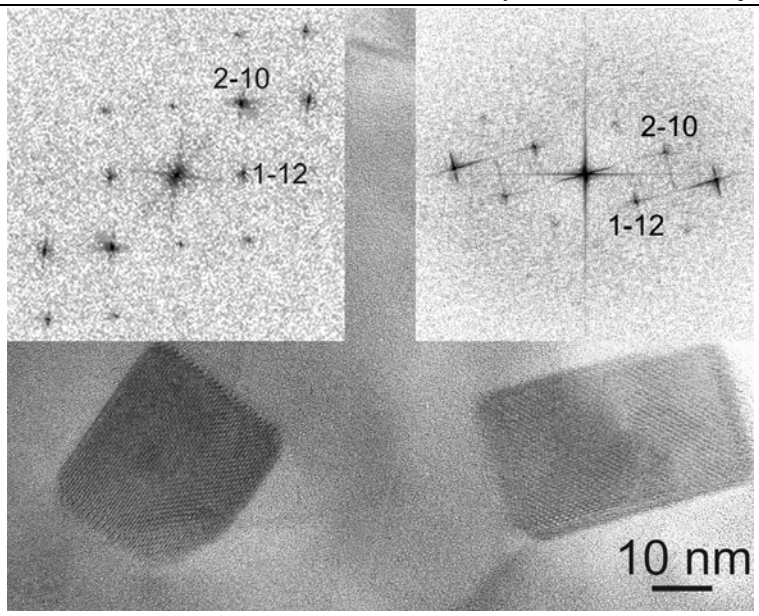

Fig. 2. HRTEM image and its Fourier transforms of specimen $Fe_{78}Si_9B_{13}$ heated at 823 K for 4h. Particles of FeB_{49} exhibiting $1\bar{1}2$ and $2\bar{1}0$ fringes are visible

Observations by means of TEM and SAED of $Fe_{78}Si_9B_{13}$ specimen heated at 823 K for 4h revealed the presence of α-Fe and Fe_2B. However, some amount of the amorphous phase was also observed after applied treatment of the specimen. Additionally, HRTEM observations showed the presence of a needle-like cuboid shaped large crystalline particles, typically between 20 and 50 nm in shorter, and even to 500 nm in elongated sizes. A magnified image of such crystallites is shown in fig. 1 with its fast Fourier transforms (FFT). The phase analysis of them was carried out by indexing the selected area diffraction patterns as well as the FFT patterns obtained from the HRTEM image of the nanocrystalline particles. The analysis results indicate that the particles with 0,742 and 0,547 lattice fringes are characteristic for $[1\bar{1}2]$ and $[2\bar{1}0]$ respectively, of the FeB_{49} compound [10]. Thus, the FeB_{49} phase, very rich in boron, was identified in the studied sample.

The structural changes are determined by parameters of the annealing and therefore the samples of the alloy were annealed at various temperatures. Investigated of the influence of these changes on the Hall effect and the electrical resistivity. The Hall resistivity ρ_H as a function of external magnetic field B_0 for samples in as-received state and samples annealed isochronally at different temperatures are presented in fig. 3. Each curve ($\rho_H = f(B_0)$) is of the typical shape as for the ferromagnetic materials and is described by means of the formula [11–14]:

$$\rho_H = R_0 B_0 + \mu_0 R_s M \,, \tag{9}$$

where: R_0 and R_s are ordinary and spontaneous Hall coefficient respectively, and M is the magnetization of the sample. This demonstrates that during the crystallization

process the macroscopic ferromagnetic ordering of the alloy is conserved. The first term of the equation (9) is the ordinary Hall resistivity ($\rho_{H0} \propto B_0 a$). It is related to the action of the Lorentz force on the current carriers and it corresponds to the slowly growing part of the $\rho_H = f(B_0)$ curve above the magnetization saturation. The second term is the spontaneous Hall effect ($\rho_{HS} \propto M$) and is represented by the initial part of the $\rho_H = f(B_0)$ curve. The ρ_{HS} is connected with a ferromagnetic state and determined by following mechanisms: a spin-orbit interaction, a skew scattering and a side jump [12]. Due to these mechanisms the mean free path of carriers decreases.

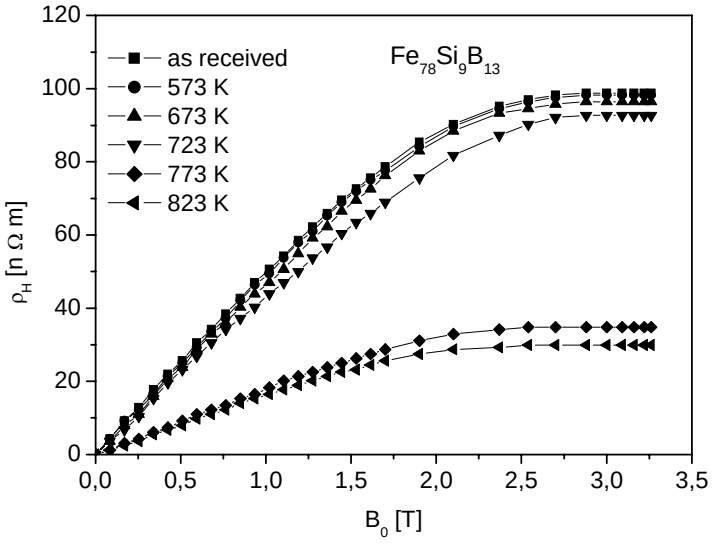

Fig. 3. The Hall resistivity, ρ_H, vs. applied magnetic induction, B_0, for samples of $Fe_{78}Si_9B_{13}$ alloy annealed at different temperatures

For the initial part of the $\rho_H = f(B_0)$ curves the spontaneous Hall coefficient R_s was calculated using the linear regression $R_s = (\partial \rho_H / \partial B_0)_{B_0 \to 0}$. Fig. 4 shows the changes of the spontaneous Hall coefficient R_s and the relative changes of the electrical resistivity (related to the resistivity of the as-received state) vs. the annealing temperature. The $\Delta\rho/\rho_0$ values show an increase in the initial range of annealing, which is connected with the structural changes of the short range ordering type. The decrease of the electrical resistivity during the crystallization is caused by the increase of the free path of the carriers in the ordered structure.

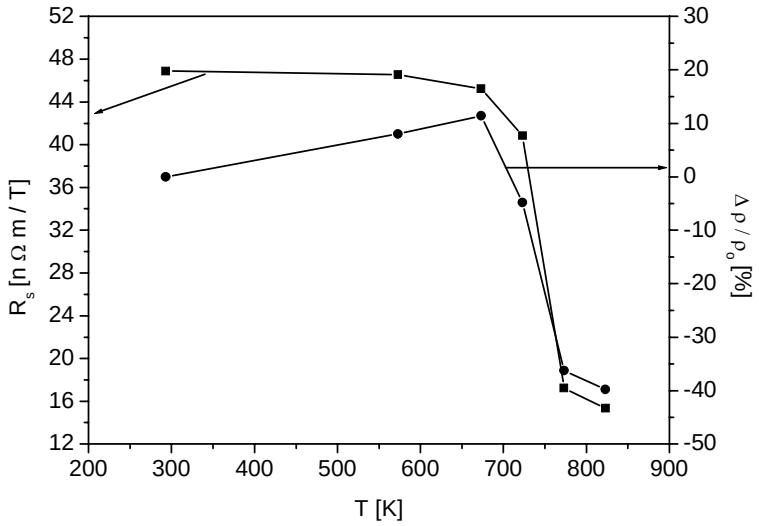

Fig. 4. The spontaneous Hall coefficient R_s and relative electrical resistivity, $\Delta\rho/\rho_0$, as a function of annealing temperature T, for the samples of $Fe_{78}Si_9B_{13}$ alloys

Berger and Bergmann gave the relationship between the spontaneous Hall coefficient R_s and the electrical resistivity ρ [14]:

$$R_S = a\rho + b\rho^2, \tag{10}$$

where: a and b are constants roughly independent of temperature.

The first term of equation (10) is responsible for the classical asymmetric scattering of charge carriers and the second term describes the quantum effect and corresponds to the lateral displacement of the charge carrier trajectory at the point of scattering , i.e. the side jump. The dependence of lg R_s on lg ρ gives the exponent k in relation $R \propto \rho^k$ and by it we can conclude which type of scattering is the dominant one for the spontaneous Hall effect. The calculated exponent k is 1,91 and this value k allows to accept that during the crystallization process the charge carriers are mainly scattered by nonclassical mechanism, i.e. side jump.

Summary of obtained results in this paper states that the crystallization of $Fe_{78}Si_9B_{13}$ metallic glass proceeds through two main stages (at 723 and 773 K). Also importance and new result is the detection of FeB_{49} nanocrystalline phase.

1. *Kissinger H.E.* Reaction kinetics in differential thermal analysis // Anal. Chem. 1957. Vol. 29. P. 1702–1706.
2. *Vázquez J, López-Alemany P.L.,Villares P.* et al. A study on non-isothermal transformation kinetics, Application to the crystallization of $Sb_{0,20}As_{0,32}Se_{0,48}$ alloy // J. Alloy Comp. 1998. Vol. 270. 179 p.

3. *Kashchiev D., Sato K.* Kinetics of crystallization preced by metastable-phase formation // J. Chem. Phys. 1998. Vol. 109. P. 8530–8540.
4. *Gao Y.Q., and Wang W.* On the activation energy of crystallization in metallic glasses // J. Non-Cryst. Solids. 1986. Vol. 81. P. 129–134.
5. *Mehta N., Kumar A.* A study of thermal crystallization in glassy $Se_{80}Te_{20}$ and $Se_{80}In_{20}$ using DSC technique // J. Therm. Anal. Cal. 2006. Vol. 83. P. 401–405.
6. *Shanker RaoT.L., Lad K.N., Pratap A.* Study of non-isothermal crystallization of amorphous $Cu_{50}Ti_{50}$ alloy // J. Therm. Anal. Cal. 2004. Vol. 78. P. 769–774.
7. *Christian J.W.,* The Theory of Transformation in Metals and Alloys, Pergamon Press, Oxford 1965.
8. *Tomaszewski P. E.* Golden Book of Phase Transitions, Wrocław 2002.
9. *Havinga E.E., Damsma H., Hokkeling P.* Compounds and pseudo-binary alloys with the $CuAl_2$ (C16)-type structure., I. Preparation and X-ray results // J. Less-Common Metals. 1972. Vol. 27. P. 169–186.
10. *Callmer B., Lundstroem T.* A single-crystal diffractometry investigation of iron in beta-rhombohedral boron // J. Sol. State Chem. 1976. Vol. 17(1–2). P. 165–170.
11. *Hurd C.M.,* The Hall Effect in Metals and Alloys, Plenum Press, New York – London, 1972.
12. *Berger L., Bergmann G.* The Hall effect of ferromagnets, in: The Hall Effect and Its Applications, C.L. Chien, C.R. Westgate (Eds.), Plenum Press, New York 1980.
13. *McGuire T. R., Gambino* R. J., *O'Handley R. C.* Hall effect in amorphous metals, in: The Hall Effect and Its Applications, C.L. Chien, C.R. Westgate (Eds.), Plenum Press, New York 1980.
14. *Stobiecki T. and Przybylski M.* Spontaneous Hall effect and magnetization of Fe-(B,Zr) and Co-Mo amorphous film // Phys. Stat. Sol. (B). 1986. Vol. 134. P. 131–139.

ДОСЛІДЖЕННЯ ВПЛИВУ КРИСТАЛІЗАЦІЇ НА ВЛАСТИВОСТІ МЕТАЛІЧНИХ СТЕКОЛ Fe-Si-B

М. Якубчик[1], П. Сіеміон[1], Л. Крайчик[2], Є. Якубчик[3]

[1]Інститут хімії і навколишнього середовища
Університет Яна Длугоша
вул. Армії Крайової 13/15, 42200 Ченстохова, Республіка Польща
[2]Інститут низькотемпературних та структурних досліджень В. Ешебіатовск
Польська Академія наук
вул. Окольна 2, 50-950 Вроцлав, Республіка Польща
[3]Інститут фізики, Університет Яна Длугоша
вул. Армії Крайової 13/15, 42200 Ченстохова, Республіка Польща

Досліджено процес кристалізації металічного скла $Fe_{78}Si_9B_{13}$ методами ДСЦ, ТЕМ, рентгенівської дифракції, вимірювання електричного опору та ефекту Холла. Унаслідок проведених вимірювань виявлено двоступеневу кристалізацію. За допомогою неізотермічних експериментів ДСК отримано енергію активації та показник Аврамі. На основі рентгенівських та ТЕМ досліджень ідентифіковані фази α-Fe(Si) та $(Fe,Si)_2B$. Результати, отримані методом ТЕМ, засвідчують

незначний вміст фази FeB_{49}, а також залишки аморфної фази. Електричний опір та опір Холла зменшуються після утворення фаз за межами аморфної матриці.

Ключові слова: металеве скло, кристалізація, енергія активації, показник Аврамі, електричний опір та опір Холла.

ИССЛЕДОВАНИЕ ВЛИЯНИЯ КРИСТАЛЛИЗАЦИИ НА СВОЙСТВЕ МЕТАЛЛИЧЕСКИХ СТЕКОЛ Fe-Si-B

М. Якубчик[1], П. Сиемион[1], Л. Крайчик[2], Е. Якубчик[3]

[1]Институт химии и окружающей среды Университет Яна Длугоша
ул. Армии Краевой 13/15, 42200 Ченстохова, Республика Польша
[2]Институт низкотемпературных и структурных исследований
В. Ешебиатовск Польская Академия наук
ул. Окольна 2, 50-950 Вроцлав, Республика Польша
[3]Институт физики, Университет Яна Длугоша
ул. Армии Краевой 13/15, 42200 Ченстохова, Республика Польша

Исследовано процесс кристаллизации металлического стекла $Fe_{78}Si_9B_{13}$ методами ДСЦ, ТЕМ, рентгеновской дифракции, измерения электрического сопротивления и эффекта Холла. В результате проведенных измерений обнаружена двухступенчатая кристаллизация. С помощью неизотермических экспериментов ДСК получена энергия активации и показатель Аврами. На основе рентгеновских и ТЕМ исследований идентифицированы фазы α-Fe(Si) и $(Fe,Si)_2B$. Результаты, полученные методом ТЕМ, подтверждают незначительное содержание фазы FeB_{49}, а также остатки аморфной фазы. Электрическое сопротивление и сопротивление Холла уменьшаются после образования фаз за пределами аморфной матрицы.

Ключевые слова: металлическое стекло, кристаллизация, энергия активации, показатель Аврами, электрическое сопротивление и сопротивление Холла.

Стаття надійшла до редколегії 04.08.2008
Прийнята до друку 25.03.2009